Prediction of dynamic mooring responses of a floating wind turbine using an artificial neural network

Prediction of dynamic mooring responses of a floating wind turbine using an artificial neural network

F A Bjørni[1], S Lien[1], T Aa Midtgarden[1]
G Kulia[2], A Verma[3], Z Jiang[1*]

1 Department of Engineering Sciences, University of Agder, N-4898 Grimstad, Norway
2 Signal Analysis Lab AS, Jon Lilletuns vei 3, N-4879 Grimstad, Norway
3 Department of Mechanical Engineering, University of Maine, USA

E-mail: zhiyu.jiang@uia.no

Abstract. Numerical simulations in coupled aero-hydro-servo-elastic codes are known to be a challenge for design and analysis of offshore wind turbine systems because of the large number of design load cases involved in checking the ultimate and fatigue limit states. To alleviate the simulation burden, machine learning methods can be useful. This article investigates the effect of machine learning methods on predicting the mooring line tension of a spar floating wind turbine. The OC3 Hywind wind turbine with a spar-buoy foundation and three mooring lines is selected and simulated with SIMA. A total of 32 sea states with irregular waves are considered. Artificial neural works with different constructions were applied to reproduce the time history of mooring tensions. The best performing network provides a strong average correlation of 71% and consists of two hidden layers with 35 neurons, using the Bayesian regularisation backpropagation algorithm. Sea states applied in the network training are predicted with greater accuracy than sea states used for validation of the network. The correlation coefficient is primarily higher for sea states with lower significant wave height and peak period. One sea state with a significant wave height of 5 meters and a peak period of 9 seconds has an average extreme value deviation for all mooring lines of 0.46%. Results from the study illustrate the potential of incorporating artificial neural networks in the mooring design process.

1. Introduction

Offshore environmental loads from wind, waves and currents depend on the climate and vary from site to site. These loads may contribute to substantial tension in the mooring lines. To ensure safe operations of floating wind turbines, design standards, e.g., [1, 2], specify that ultimate, fatigue, and accidental limit states be considered for mooring design, and coupled numerical simulations of wind turbines be carried out. As many design load cases are required for the time-consuming simulations, there is a need to reduce the total number of simulations without loosing the accuracy of the predicted mooring tensions and other structural responses. In this paper, we hypothesise that with the application of machine learning methods the computational effort used during the design and analysis could be greatly reduced. The current paper investigates the effect of machine learning methods on predicting the mooring line tension of a spar floating wind turbine. By Machine learning (ML), we refer to algorithms that make successive predictions based on previous experience [3]. The ML-approach explored in this paper is a shallow artificial neural networks (ANN) [4]. Its application in mathematical modelling, optimisation, pattern recognition, and image processing have been greatly explored in the past decade after the

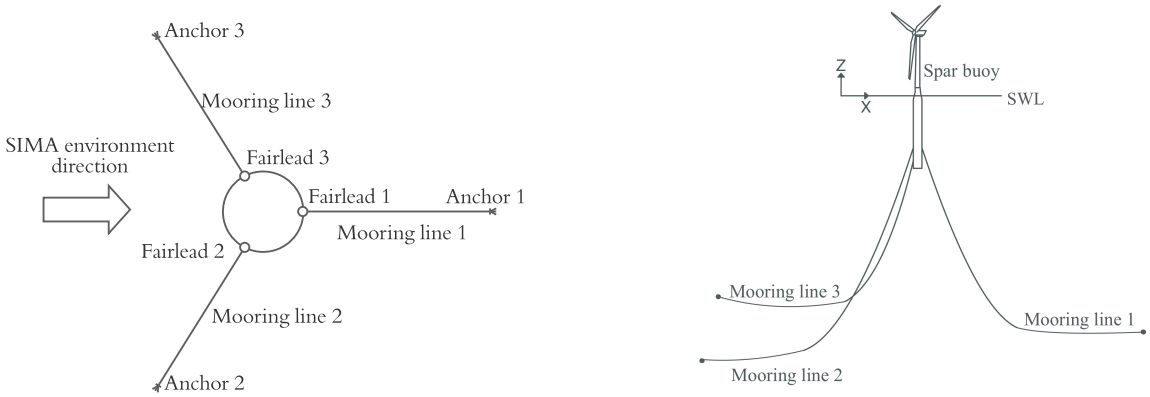

(a) Mooring line structure.

(b) Side view of the floating wind turbine system.

Figure 1: Schematic of the mooring layout and the OC3-Hywind wind turbine

emergence of cheaper parallel computing, making it possible to use it for greater data sets. ANN is built up of an input layer of artificial neurons (or neurons), hidden layers with neurons, and a final layer of output neurons.

ANN has been applied to a wide range of offshore bottom-fixed and floating structures in recent years. For example, Guo et al. [5] considered ANN in constructing the response surface for solving a damage identification problem of a jacket structure. Sdarta et al.[6] used an ANN model with two hidden layers for predicting the time series of mooring line tension for a semi-submersible platform. It was concluded that ANN can be applied to reproducing time series that are both incorporated and not incorporated in the training, with sufficient accuracy. Li and Choung [7] illustrated that a multi-layered ANN model can predict the wide-banded fatigue damage in the mooring lines of a semi-submersible floating offshore wind turbine with good accuracy. However, because of the first- and second-order wave loads on floating structures [8], mooring tensions will experience small and large cycles of different periods, it can be challenging to predict the entire time series of mooring line tension. To address this challenge, this paper considers an application of the ANN with Bayesian regularisation backpropagation algorithm to predict the time-varying processes of dynamic mooring tensions under wave-only conditions. The results of this paper contribute to efficient prediction of structural responses from numerical simulations of floating wind turbines and can be extended to facilitate fatigue analysis of mooring lines with reduced number of simulations. The paper is structured as follows. Sec. 2 describes the numerical model of the spar floating wind turbine, the ANN setup, and the test and training cases. Sec. 3-5 present the results. Finally, Sec. 6 draws the concluding remarks.

2. Description of the numerical model and training cases

The OC3-Hywind model [9] is a spar floating wind turbine (FWT) which consists of a slender spar buoy, a 5-megawatt wind turbine, and three catenary mooring lines. From the platform base up to the still water level, the model has a draft of 120 m, and the platform top lies 10 m above the still water level. Figure 1 shows top and side views of the FWT with moorings. In this study, waves are propagating along the x-axis.

2.1. Simulation of the floating wind turbine

SIMA [10, 11] is a time-domain simulation tool for calculating and analysing multibody floating systems. SIMA is used to model the OC3-Hywind in this study. Using this model, we first carry out numerical free decay tests of the FWT in still water for calculating the eigenperiods and for

Table 1: List of the platform natural periods obtained from the numerical free decay test.

Motion	Natural period [s]
Heave	31.23
Surge	124.97
Sway	124.97
Yaw	8.23
Roll	29.90
Pitch	29.90

verifying the model. The natural periods of the mooring wind turbine are listed in Table 1 and the differences for all six degrees of freedom (DOF) are within 2.4% deviation from the reference values [9].

Then, dynamic analysis of the FWT is performed in irregular waves for different sea states. The JONSWAP wave spectrum [12] with a peakness parameter γ of 3.3 is applied to generate the irregular waves. The wind loads are not included in this study for simplicity. Each numerical simulation last 2200 seconds, where the first 400 seconds is discarded in postprocessing due to the start-up transient. The computational time of each is approximately 600 seconds.

2.2. Data selection for training, validation and testing

Table 2 describes the range of sea state parameters, significant wave height (H_s) and wave spectral peak period (T_p). As shown, H_s ranges between 1 and 8 m and T_p between 5 and 16 s, covering high probability of occurrence of typical North Sea sites. Among the symbols, $V_1 ... V_{12}$ represents the first to the 12^{th} validation data sets. $T_1 ... T_{20}$ represents the first to the 20^{th} training data sets. The entire combination of H_s and T_p in the validation set is not overlapping, but within the range of those in the training set. This is because ANN can interpolate based on the training data, but cannot extrapolate. Separate data sets are withheld from the training process to validate the model and test its performance.

The model is trained by providing time series with six DOF of the platform motions in 60-seconds intervals as input. Time series of the corresponding mooring line axial force is used as training output of the network. A sliding window is applied to both input and output data to limit the complexity of the prediction, and thus increasing the yield of the network. An illustration of how sliding window is applied is shown in Figure 3. The use of sliding windows

Table 2: Data corresponding to the training and validation sea states T : training, V: validation.

	T_p [s]						
H_s [m]	5	6.5	9	13	14	15	16
1	T_1		T_6		T_{11}		T_{16}
1.5		V_1		V_5		V_9	
2	T_2		T_7		T_{12}		T_{17}
2.5		V_2		V_6		V_{10}	
3	T_3		T_8		T_{13}		T_{18}
4		V_3		V_7		V_{11}	
5	T_4		T_9		T_{14}		T_{19}
7		V_4		V_8		V_{12}	
8	T_5		T_{10}		T_{15}		T_{20}

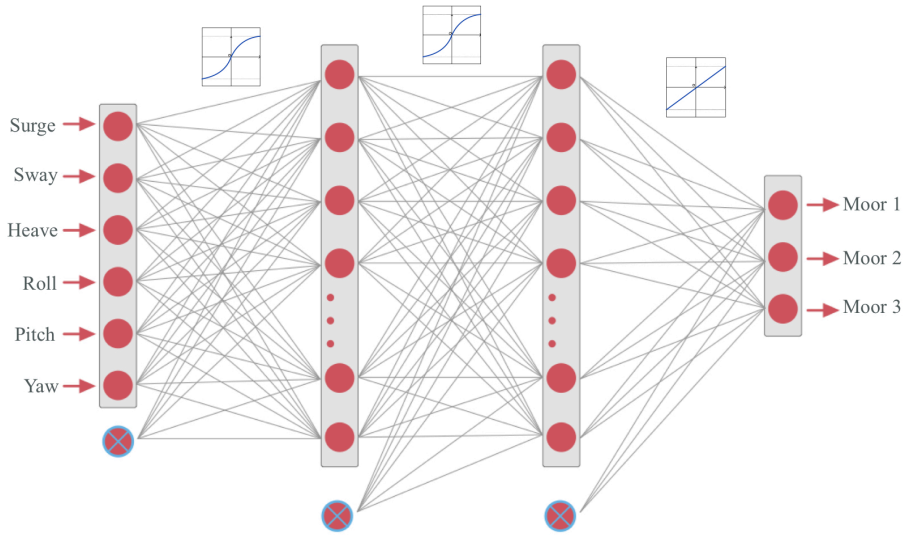

Figure 2: Layer architecture of the ANN.

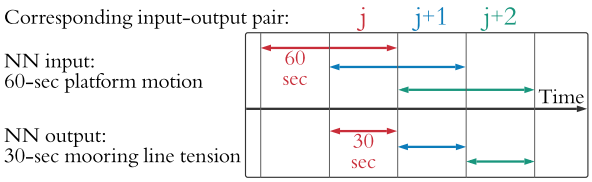

Figure 3: Application of sliding windows to the time series.

follow a similar principle and motivation as a convolutional neural network [4]. In future work, it is recommended to explore the use of overlapping sliding windows convoluted with a window function [13].

The network layer architecture is shown in Figure 2 and consists of an input layer with the width of 360, two hidden layers with 35 neurons each, and an output layer with width 90. The network is considered shallow as there are only two layers.

The hidden layers consist of interconnected neurons arranged. The neurons in each layer are attached to the neurons in the successive layer. The connections between the neurons carry an associated weight. These weights are adjusted when training the neuron to minimise the difference between the predicted $\hat{y}$, and the actual y. In this network, the Pearson correlation coefficient is used to calculate this value, hereafter referred to as the R-value and is given in equation (1).

$$R(y,\hat{y}) = \frac{1}{N-1}\sum_{n=0}^{N-1}\left(\frac{y[n]-\overline{y}}{\sigma_y}\right)\left(\frac{\hat{y}[n]-\overline{\hat{y}}}{\sigma_{\hat{y}}}\right), \tag{1}$$

where $y[n]$ and $\hat{y}[n]$ are the discrete time-signals with length N, and mean values $\overline{\hat{y}}$, $\overline{y}$ and standard deviations σ_y, $\sigma_{\hat{y}}$, respectively.

The Bayesian regularisation backpropagation is used for training, i.e., updating the weights so that it yields good predictions for all or most of the training data [14, 15]. A flowchart of the calculation of the principles in the Bayesian regularisation backpropagation is displayed in

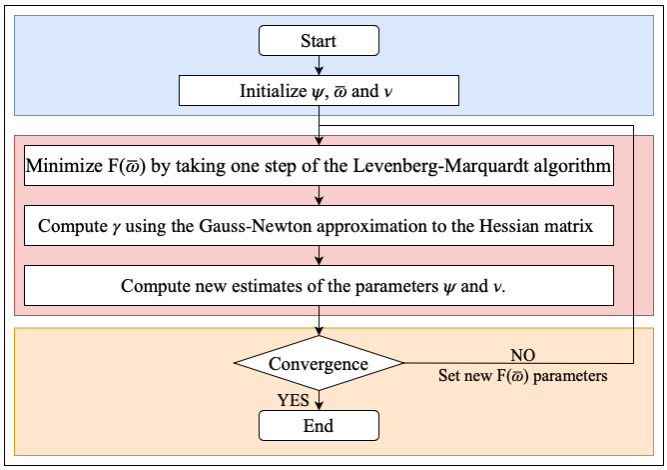

Figure 4: Flowchart of the training procedure of the Bayesian regularisation backpropagation algorithm [16]

Figure 4. The computational time needed to train the ANN is is over 270 hours for a personal computer with a CPU of 64 GB memory and 2.59 GHz. In contrast, when predicting the outputs using the ANN, the computational time is only a few seconds.

The hyperbolic tangent sigmoid transfer function $\phi[n]$ is chosen as the activation function in all neurons and is shown in equation (2) [17].

$$\phi[n] = \frac{2}{1 + e^{-2n}} - 1 \tag{2}$$

After the last hidden layer, a linear activation function is used. The output of the last linear activation function is the resulting prediction, $\hat{y}$. The network architecture is chosen in this study based on a exploratory study of several network types. A more rigorous approach or the use of a deep network might yield more precise predictions and is recommended for future work.

3. Comparison of the training sea states

Figure 5a compares the average R-value—as defined in Equation 1—computed for the three different sets of training when tested on the training sea states. The average R-value shows that the ANN model performs better for some types of sea states. Figure 5b shows how the ANN model with 35 hidden neurons can predict the three different mooring lines for each training sea state. For all sea states, some variation between each mooring line can be seen, but lines 2 and 3 repeatedly follow the same pattern, while line 1 overall performs slightly superior.

For evaluating how well the ANN model with 35 hidden neurons can predict the pattern of the target values, both the target values from SIMA and the computed output values from the ANN are plotted together.

Figure 6 displays a time series for the sea state with an H_s of 3 m and a T_p of 5 s. Some deviation is observed in the high-frequency responses corresponding to the peak period, notably line 2 and line 3, with tension peaks reaching a deviation of 1.6%. For the OC3-Hywind model, the platform's surge natural period is 124.3 seconds which can be observed in the figure. All time series displays high-frequency noises. In general, the computations from the ANN can predict the dominant patterns of the mooring line tension. The trained ANN model can accurately predict the low-frequency response of the tension, corresponding to the platform's surge natural periods. Addition of the input data can be done to prevent these difficulties, both by extending the current data sets and by considering additional sea states in the training.

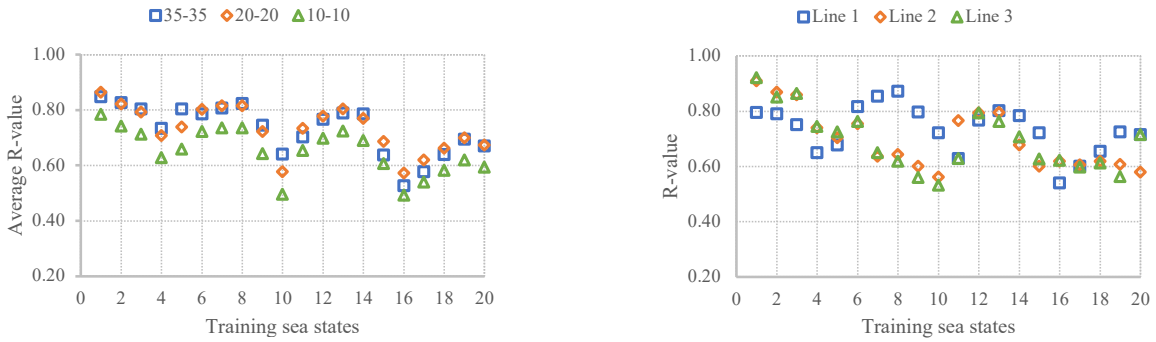

(a) Average correlation coefficient with different number of neurons.

(b) Correlation factor of three mooring lines (ANN structure: 35-35).

Figure 5: Variation of the R-value for the training sea states

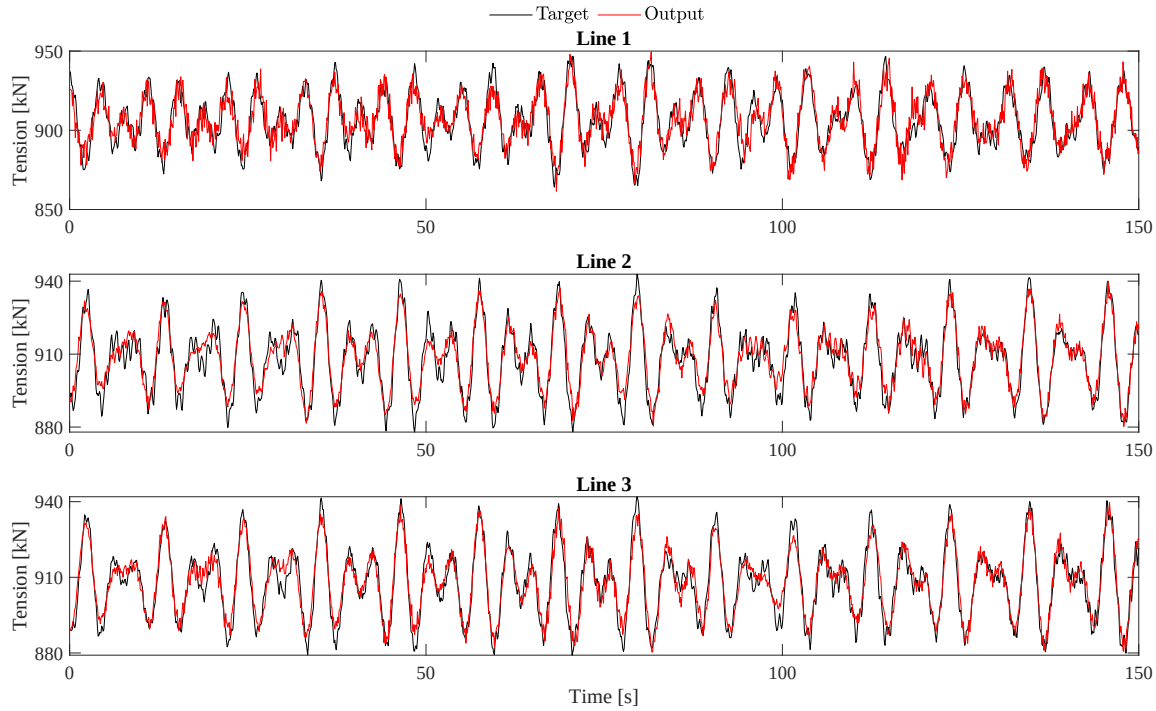

Figure 6: Time series of mooring line tension (H_s=3 m, T_p=5 s, [250–400 s]).

4. Comparison of the validation sea states

Figure 7a compares the average R-value computed for the three different networks when tested on the validation sea states. Overall, the R-value indicates that the ANN model performs less satisfactorily adapting to sea states not used in the training set. The validation set obtains a correlation coefficient which is 0.06 below the value obtained with the training set.

Figure 7b shows how the ANN model with 35 hidden neurons can predict the three different mooring lines for each of the validation sea states. As observed with the training set, some variations can be observed between the mooring lines, but line 2 and line 3 have similar observations. Different from the training set, line 1 performs inferior for the validation sets

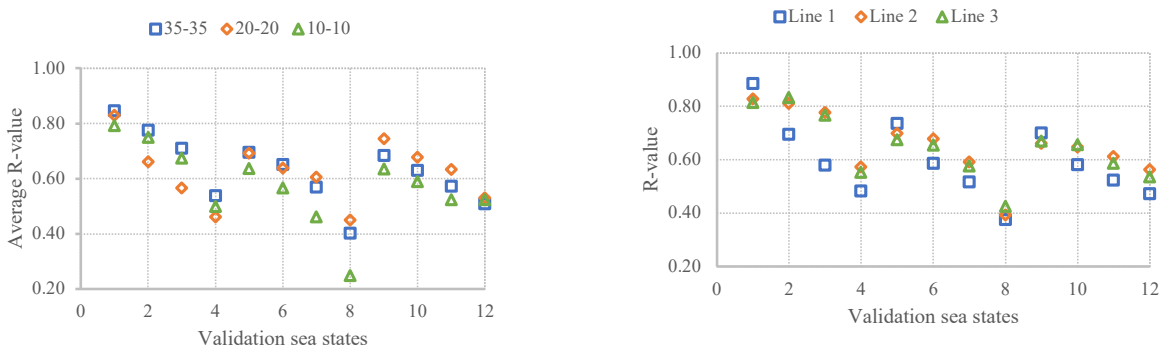

(a) Average correlation coefficient with different number of neurons.

(b) Correlation factor of three mooring lines (ANN structure: 35-35).

Figure 7: Variation of the R-value for the validation sea states

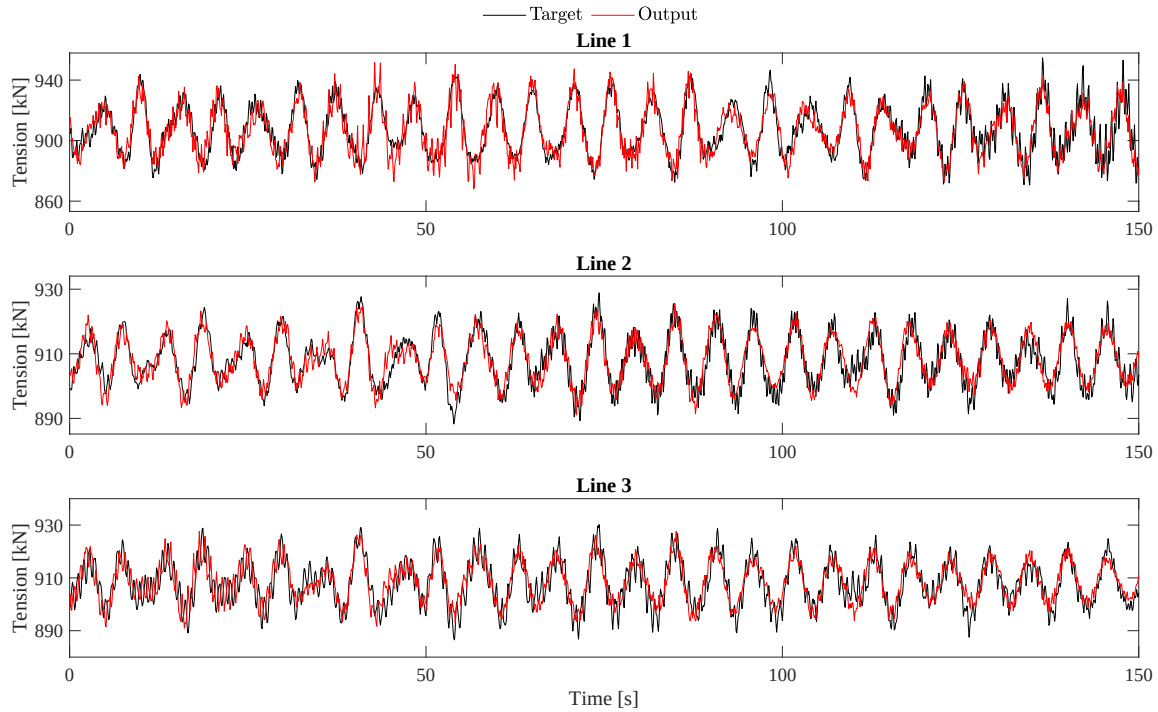

Figure 8: Time series of mooring line tension (H_s=2.5 m, T_p=15 s, [1500–1650 s]).

for all the sea states except for the sea states 1, 5, and 9 which all have the wave height of 1.5 meters. By comparing the R-values calculated for the validation set and the R-values from the training set, a lower correlation factor for the validation set can be observed.

Figure 8 and Figure 9 display appreciable fluctuations in the noise and correlation of target and output values. Because of their symmetry with regard to the wave direction, line 2 and line 3 show a resemblance as observed in the training set, but the amount of noise between the target values for the two lines appears to differ more significantly than perceived in the training set. The ANN model has recognised difficulty predicting the noise for line 2 and line 3.

The ANN accurately predicts the low-frequency part of the tension corresponding to the

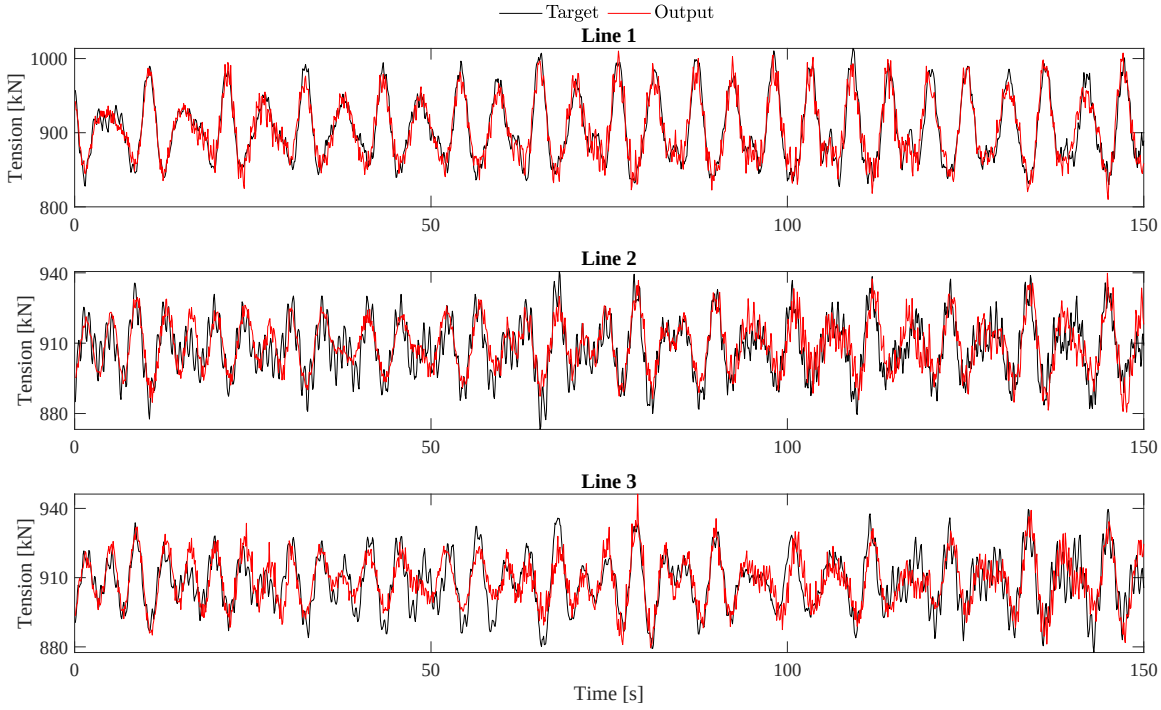

Figure 9: Time series of mooring line tension (H_s=1.5 m, T_p=6.5 s, [350–500 s]).

platform's surge motion but shows slight deficits in the high-frequency wave peaks. Different from the training sets is that the validation figures show a worse prediction of the noisiest parts of the time series. For some parts of the sea states and especially for line 1, it can be observed that the ANN output predicts a noisier time series than the SIMA output. This can be due to the deteriorated R-value for line 1 for many of the sea states. In general, the ANN model is observed to interpolate between the training sea states and use the gathered information to predict sea states not used in the training process. For the noisy vibration signals and the wave-frequency part of the mooring tension, the performance of the ANN prediction deteriorates. It remains a question how these deviations affect the fatigue lifetime estimate.

5. Time series analysis

Regression tools for better examining the ANN prediction accuracy are utilised. These analyses are performed to evaluate if the ANN model manages to accurately predict the main patterns in the mooring line tension, even if it has difficulties with the noisy and high-frequency vibrations. To confirm that the linear regression had not altered the time series, the average between the target and output value for each mooring is calculated for both the original and the regression time series. This calculation indicates minor differences and thus demonstrates that the linear regression is consistent with the time series, and the calculated values are displayed in Table 3.

Figure 10 shows the time series of sea state 9 after being processed through linear regression. The linear regression has removed the short-span noise for all three lines and left the main pattern. It can be observed that the ANN model is predicting the values precisely and only missing a few of the extrema.

The ANN model can predict the tension extremes which are compared for the whole time series. These analyses are performed for one training sea state 9 (H_s=5 m, T_p=9 s). All the

Table 3: Comparison of the original time series (Figure 9) and the regression analysis.

Line	Original [kN]	Regression [kN]	Difference [%]
1	1.51	1.54	-1.99
2	1.07	1.05	1.87
3	0.29	0.28	3.45

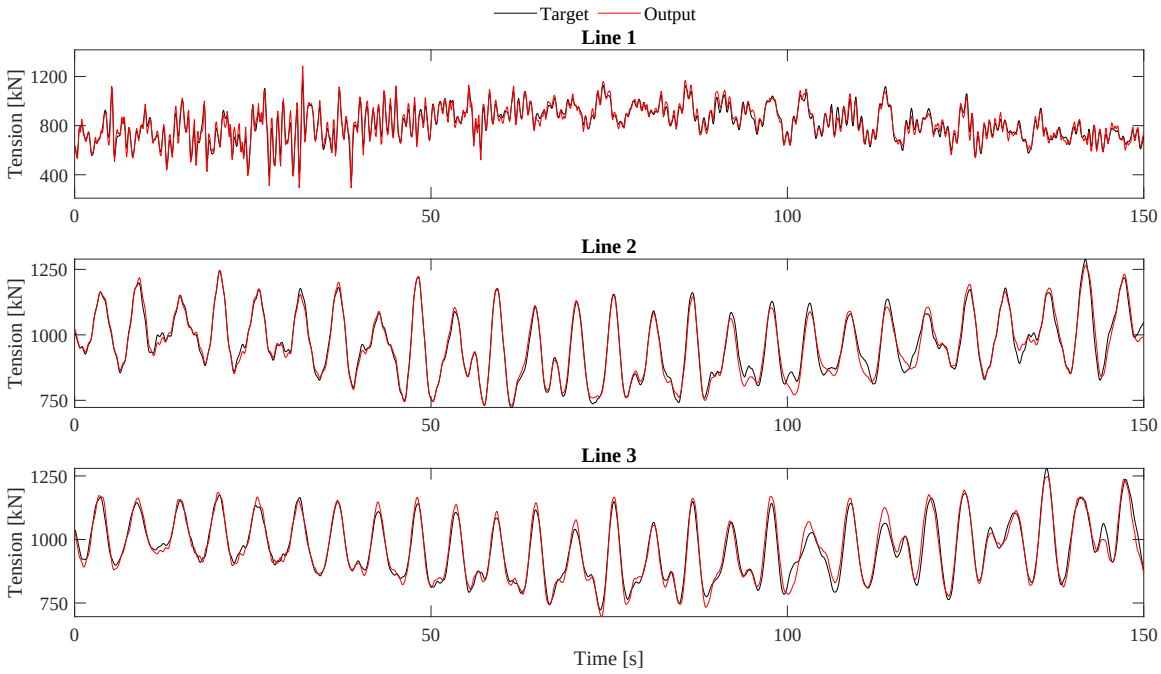

Figure 10: Smoothed time series of mooring line tension for sea state V(9) (H_s=1.5 m, T_p=15 s, [0–150 s]).

Table 4: Percentage difference of the extreme mooring line tension

	Time Interval [s]												
	0-150	150-300	300-450	450-600	600-750	750-900	900-1050	1050-1200	1200-1350	1350-1500	1500-1650	1650-1800	Avg.
Line 1	0.48%	0.59%	0.46%	0.74%	0.27%	0.67%	0.75%	0.37%	0.76%	1.08%	0.43%	0.65%	0.64%
Line 2	0.09%	0.41%	0.17%	0.38%	0.35%	0.41%	0.29%	0.55%	0.35%	0.31%	0.39%	0.37%	0.34%
Line 3	0.16%	0.27%	0.09%	0.14%	0.31%	0.26%	0.53%	0.62%	0.57%	0.78%	0.85%	0.34%	0.41%
Avg.	0.24%	0.42%	0.24%	0.42%	0.46%	0.45%	0.53%	0.51%	0.56%	0.72%	0.56%	0.45%	0.46%

obtained tension extremes are manually filtered to ensure that the obtained peaks are not too closely correlated, i.e., the period interval between two adjacent peaks must exceed 0.5 seconds. In Table 4, all the calculated deviation in the extremes is presented as an average value for each of the time intervals. For this specific sea state, a higher deviation for mooring line 1 can be observed. The highest deviation can be observed in the time interval 1350-1500 s, with the highest value reaching a deviation of 1.08%. The uppermost deviation calculated for any single value in this specific sea state was 1.67%. For designing mooring lines according to DNV-OS-E301 [18], the ultimate mooring tension is a primary consideration, and the extreme line tension deviations in the ANN prediction should be as small as possible.

6. Concluding remarks

This paper outlines how a shallow artificial neural network can be used to predict the mooring line tension. The OC3-Hywind floating wind turbine is used as a case study where wave-only simulations are considered. The network predicted the time series with 71% accuracy, using the Pearson correlation as a success criterion. The avarage extrema deviation of the training sea state where the wave height is 5 m and spectral peak period of 9 s is 0.46%. Application of an artificial neural network model to predict mooring line tension can potentially provide a substantial improvement in the calculation efficiency of real-time stress, fatigue life, and ultimate load in the mooring lines of marine structures. Although this work does not consider wind loads, an application of this method combined with wind-wave loading conditions can be pursued in future, and design load cases in operational, parked, and transient conditions can be considered.

Acknowledgments

The financial support of UH-nett Vest (project number 720025) is gratefully acknowledged.

References

[1] DNV GL. *Standard DNV-ST-0119 Floating wind turbine structures*, 2018.
[2] DNV. *Recommended Practice: DNVGL-RP-0286 Coupled analysis of floating wind turbines*, 2020.
[3] M Yousef and J Allmer. *miRNomics: MicroRNA Biology and Computational Analysis*. Springer Science+Business Media, New York, 2014.
[4] Y LeCun, Y Bengio, and G Hinton. Deep learning. *Nature*, 521:436–444, 05 2015.
[5] J Guo, J Wu, J Guo, and Z Jiang. A damage identification approach for offshore jacket platforms using partial modal results and artificial neural networks. *Applied Sciences*, 8(11):2173, 2018.
[6] DE Sidarta, J Kyoung, J O'Sullivan, and KF Lambrakos. Prediction of offshore platform mooring line tensions using artificial neural network. In *International Conference on Offshore Mechanics and Arctic Engineering*, volume 57632, page V001T01A079. American Society of Mechanical Engineers, 2017.
[7] CB Li and J Choung. Fatigue damage analysis for a floating offshore wind turbine mooring line using the artificial neural network approach. *Ships and Offshore Structures*, 12(sup1):S288–S295, 2017.
[8] L Zhang, W Shi, M Karimirad, C Michailides, and Z Jiang. Second-order hydrodynamic effects on the response of three semisubmersible floating offshore wind turbines. *Ocean Engineering*, 207:107371, 2020.
[9] J Jonkman and W Musial. Offshore Code Comparison Collaboration (OC3) for IEA Wind Task 23 Offshore Wind Technology and Deployment. 303, 01 2010.
[10] MARINTEK. *SIMO Theory Manual Version 4.8.4*, 2016.
[11] IJ Fylling, CM Larsen, N Sødahl, H Ormberg, A Engseth, E Passano, and K Holthe. RIFLEX theory manual. Technical report, SINTEF report no. STF70 F, 1995.
[12] KF Hasselmann, TP Barnett, E Bouws, H Carlson, DE Cartwright, K Eake, JA Euring, A Gicnapp, DE Hasselmann, P Kruseman, et al. Measurements of wind-wave growth and swell decay during the joint north sea wave project (JONSWAP). *Ergaenzungsheft zur Deutschen Hydrographischen Zeitschrift, Reihe A*, 1973.
[13] A Nuttall. Some windows with very good sidelobe behavior. *IEEE Transactions on Acoustics, Speech, and Signal Processing*, 29(1):84–91, 1981.
[14] DJC MacKay. Bayesian interpolation. *Neural computation*, 4:415–447, 11 1992.
[15] F D Foresee and M Hagan. Gauss-newton approximation to bayesian learning. *Proceedings of International Conference on Neural Networks (ICNN'97)*, 3:1930–1935 vol.3, 1997.
[16] ZYue, Z Songzheng, and L Tianshi. Bayesian regularization BP neural network model for predicting oil-gas drilling cost. *2011 International Conference on Business Management and Electronic Information*, 2:483–487, 2011.
[17] TP Vogl, JK Mangis, AK Rigler, WT Zink, and DL Alkon. Accelerating the convergence of the back-propagation method. *Biological Cybernetics*, 59:257–263, 1988.
[18] DNV GL. Offshore standard DNV-OS-E301 position mooring, 2008.